Steady-state measurements of ternary mixtures in thermogravitational microcolumn using optical digital interferometry

Berin Šeta[1], Estela Lapeira[2], Jna. Gavalda[1], M. Mounir Bou-Ali[2], Xavier Ruiz[1]

[1]Universitat Rovira i Vigili, Tarragona, Spain,
[2] Mondragon Unibertsitatea, Mondragon, Spain;
berin.seta@urv.cat
mbouali@mondragon.edu

Correspoding author: Berin Šeta, berin.seta@urv.cat, telephone number: +34 977558107; fax: +34 977558237

Abstract

Steady-state measurements in a thermogravitational microcolumn using optical digital interferometry are presented here for the first time in the literature in the case of ternary mixtures. These measures enabled the subsequent obtaining of thermodiffusion coefficients of a ternary mixture once convection reaches the steady-state. The ternary mixture used was the benchmark one, tetrahydronaphthalene (THN) – isobutylbenzene (IBB) and n-dodecane (nC12) with mass fraction of 0.8-0.1-0.1 respectively. Contrast factors due to the change in the concentration field were measured and compared with the corresponding ones in the literature. Uncertainty in the results was found to be of similar order of magnitude as in the case of Selectable Optical Diagnostic Instrument (SODI), which means that the condition number of that contrast factor matrix is almost equal to the present one. Final values of thermodiffusion coefficients were compared with the results reported from other optical techniques, as well as with the results obtained by the traditional long opaque thermogravitational columns (TGC). Some proposals were then made in order to improve accuracy reducing the condition number of the contrast factor matrix.

Introduction

Thermodiffusion plays an important role in many technological and biological processes of separation (Bou-Ali et al 1998; Kozlova et al. 2016; Khouzam et al. 2012; Martin-Mayor et al. 2018). Most of the systems found in nature are multicomponent but only the simplest, the ternary ones, will be the focus of this work. In the literature, it is possible to find many data about thermodiffusion in the case of binary mixtures (Lapeira et al. 2018; Šeta et al. 2019a; Šeta et al. 2020; Ning et al. 2006; Lapeira et al. 2016; Lapeira et al. 2017), while the interest in ternary mixtures recently started (Larranaga et al. 2014a; Blanco et al. 2010; Selechynh et al. 2013, Šeta et al. 2019b). Experimental techniques capable of measuring thermodiffusion/Soret coefficients in these ternary systems are, Optical Digital Interferometry (ODI) (Mialdun et al. 2013), Optical Beam Deflection Technique (OBD) (Königer et al. 2010), Rayleigh-Bénard configuration (Larre et al.

1997) and thermogravitational techniques (TGC) (Leahy-Dios et al. 2005). All those techniques are applied on earth laboratories and their results compared with the ones obtained by the SODI instrument in the International Space Station under microgravity conditions (Ahadi et al. 2016; Galand et al. 2016; Bou-Ali et al. 2015; Mialdun et al. 2019).

In the case of thermogravitational techniques, traditional opaque thermogravitational column is used to determine thermodiffusion coefficients in the ternary mixtures (De Mezquia et al. 2012; Larranaga et al. 2014b; Errarte et al. 2019). Analysis with traditional column combined measurements of refractive index and density along column height in the steady state after mixture sampling. Nevertheless, in this work an optical digital interferometry is proposed for the first time to analyze thermodiffusion in microcolumn for ternary mixtures via in situ and non invasive analysis. In this way, new methodology opens possibility to analyse signal in both transient and steady state regime. For this article, focus is only on the steady-state measurements. Once the separation in the microcolumn reached the steady-state, the vertical differences between the refractive indexes of two different wavelengths have been used to evaluate the vertical difference of concentration and consequently the thermodiffusion/Soret coefficient (Naumann et al. 2012). The new analysis has some advantages over the traditional one including, i) easier evaluation of the transient part of the separation process, ii) small sample size –which is especially important in case of rare and biological fluids- and iii) no need for sampling extraction perturbing the flow conditions in the mixture, iiii) it enables analysis along all the height of the column. However the validation of the thermodiffusion coefficients in the ternary systems is a much more complex issue than in the binary ones, due to several problems inherent to the measures in the optical properties which strongly deviate the coefficients. For that reason, to obtain thermodiffusion/Soret coefficient we have used our own experimental data but also other optical properties of the different groups (Mialdun et al. 2017).

Experimental details

The dimensions of the thermogravitational microcolumn used are $d = 0.51$mm, $L = 30$mm and $b = 3$mm, where d is the gap between walls on which temperature is imposed, h the height along which the concentration difference is measured and b is breadth of column. This means that the microcolumn has an aspect ratio $A = \frac{L}{d} \approx 60$ and a small volume, nearly 50 μL. Figure 1 displays the microcolumn used on the left side, while traditional thermogravitational column is shown in the middle where sample extractions are obligatory for the determination of thermodiffusion coefficients. In order to validate the results of this new technique, the benchmark tetrahydronaphthalene (THN) / isobutylbenzene (IBB) / n-dodecane (nC12) mixture was used with values of mass fraction 0.8 / 0.1 / 0.1. Purity of chemicals used was for THN (purity, 98+%), IBB (purity, 99%) and nC12 (purity, 99%). Filling has been done manually, slowly introducing liquid into microcolumn from the bottom to the top using 2 ml syringes. Injection was carried

out carefully in order to avoid formation of bubbles in the liquid. In the manuscript THN will be considered as c_1, IBB as c_2 and nC12 as c_3. This choice was due to its gravitational stability, since all binary pairs exhibit positive Soret behaviour, but also due to the possibility to compare the thermodiffusion coefficients with other groups that used non-convective techniques (OBD and ODI) in Earth conditions and with SODI in microgravity conditions. Finally a He-Ne red laser with 633 nm wavelength and an Excelsior Diode-pumped blue laser with 473 nm wavelength were used for measurements in optical digital interferometry.
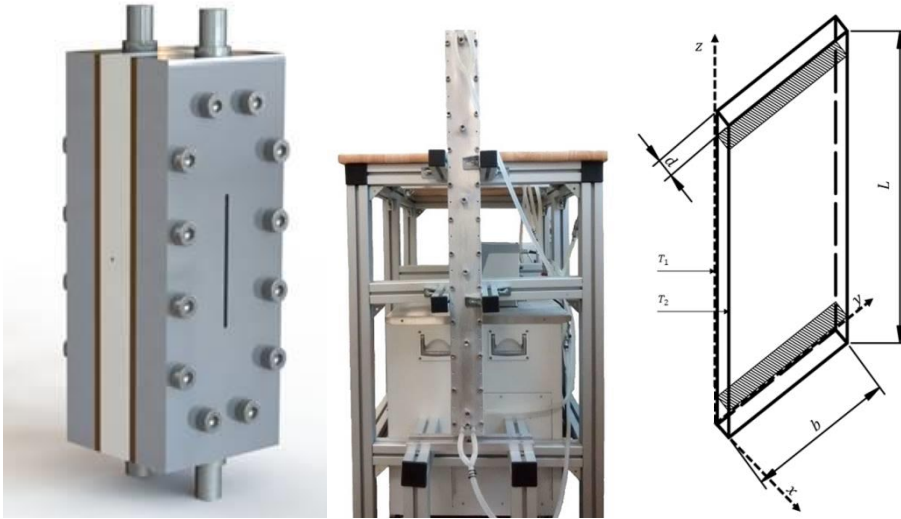

Figure 1: Visual appearance of microcolum (left), traditional thermogravitational column (middle) and sketch of microcolumn (right)

Experimental methodology

The most important step in the evaluation of the thermodiffusion coefficients using optical techniques is the determination of the contrast factors. In order to determine them, we measured the refractive index of different mixtures with slightly different concentrations around the mean concentration of 0.8/0.1/0.1 for different wavelengths. This concentration has been bolded in the Table 1. As an example, Table 1 shows the density and refractive indexes on two wavelengths obtained for twenty five mixtures. References (Blanco et al. 2010; Leahy-Dios et al. 2005) explain in detail how the contrast factors are obtained in the traditional long opaque thermogravitational columns.

Mass fraction of THN	Mass fraction of IBB	Mass fraction of nC12	ρ (density) [kg/m³]	n_D (refractive index, λ=633nm)	n_D (refractive index, λ=480nm)
0.8797	0.0607	0.0596	940.728	1.523634	1.538062
0.8597	0.0806	0.0597	938.064	1.522497	1.536877

0.8403	0.0997	0.0601	935.717	1.521348	1.535679
0.8198	0.1203	0.0599	933.172	1.520210	1.534492
0.7993	0.1400	0.0608	931.257	1.519039	1.533264
0.8592	0.0608	0.0800	934.985	1.520637	1.534831
0.8393	0.0807	0.0799	932.849	1.519621	1.533789
0.8203	0.1000	0.0798	930.328	1.518673	1.532807
0.8021	0.1185	0.0795	928.242	1.517316	1.531385
0.7788	0.1401	0.0811	925.821	1.516051	1.530048
0.8390	0.0599	0.1011	930.050	1.517598	1.531568
0.8195	0.0799	0.1006	927.060	1.516589	1.530535
0.8002	**0.1000**	**0.0999**	**925.348**	**1.515588**	**1.529486**
0.7762	0.1235	0.1002	922.871	1.514242	1.528082
0.7607	0.1395	0.0997	920.503	1.513614	1.527429
0.8195	0.0609	0.1196	924.792	1.514937	1.528712
0.8001	0.0800	0.1199	922.519	1.513841	1.527566
0.7786	0.1003	0.1211	920.032	1.512547	1.526219
0.7592	0.1213	0.1196	917.521	1.511591	1.525225
0.7400	0.1407	0.1194	915.460	1.510791	1.524397
0.7996	0.0613	0.1391	918.783	1.512244	1.525828
0.7790	0.0814	0.1395	917.232	1.510987	1.524502
0.7607	0.0996	0.1397	914.783	1.509992	1.523474
0.7389	0.1207	0.1404	912.579	1.508743	1.522160
0.7203	0.1407	0.1390	910.344	1.507871	1.521250

Table 1: Density and refractive index measurements for 25 different mixtures around benchmark composition of 0.8/0.1/0.1 on wavelengths 633nm and 480nm

The difference between these procedures and the ones used in the present work is related with the level of information extracted of the experiment. In traditional columns, the sample extraction at certain number of points enables the simultaneous measurement of the density and the refractive index at one wavelength. On the contrary, in the present case, the experimental data is related with the refractive index only.

Specifically, in the microcolumn, planes of refractive index values can be obtained for a wavelength λ, with a_0, a_1, a_2 the calibration fitting parameters, as a function of the mass fractions c_1, c_2 are mass fractions of the two independent components in Eq. 1.

$$n(\lambda) = a_0 + a_1 c_1 + a_2 c_2 \quad (1)$$

The mass fraction of the third dependent component is found simply by $c_3 = 1 - c_1 - c_2$. As an example Fig. 2 and Fig. 3 show the refractive index values along different compositions obtained for the two different wavelengths. Finally the values of the corresponding contrast factors can be simultaneously evaluated from the slopes of these planes. In the present work we also measured contrast factors for the rest of the available wavelengths in the Anton Paar multiwavelength refractometer. The values of the plane fitting parameters for each value can be found in Table 2.
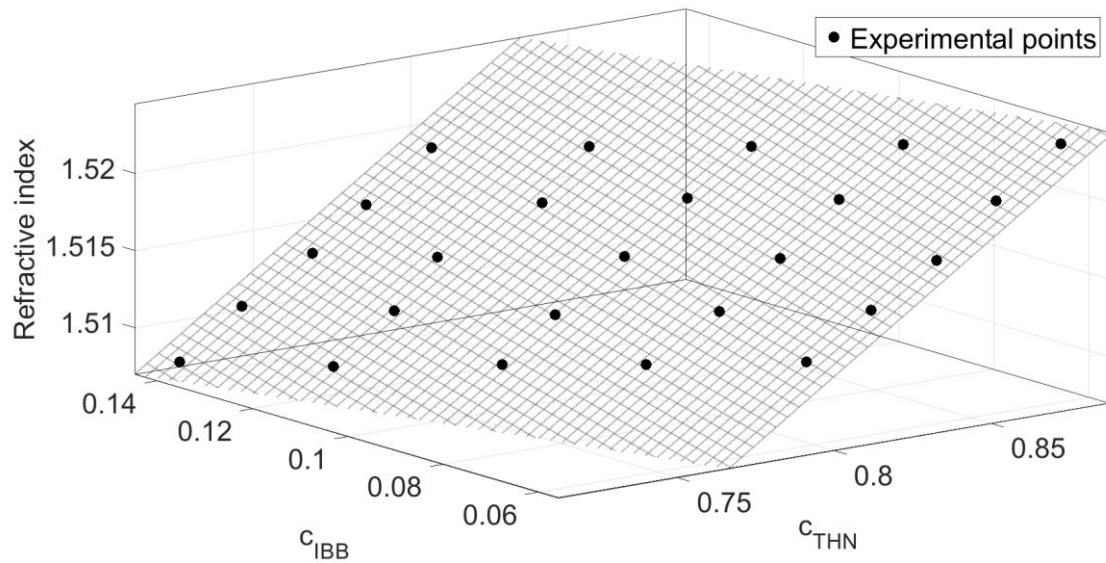
Figure 2: Fitting plane with experimental points from Table 1 at the wavelength of 633nm. C_{IBB} and C_{THN} axes represent mass fraction of isobutylbenzene and tetrahydronaphthalene respectively.
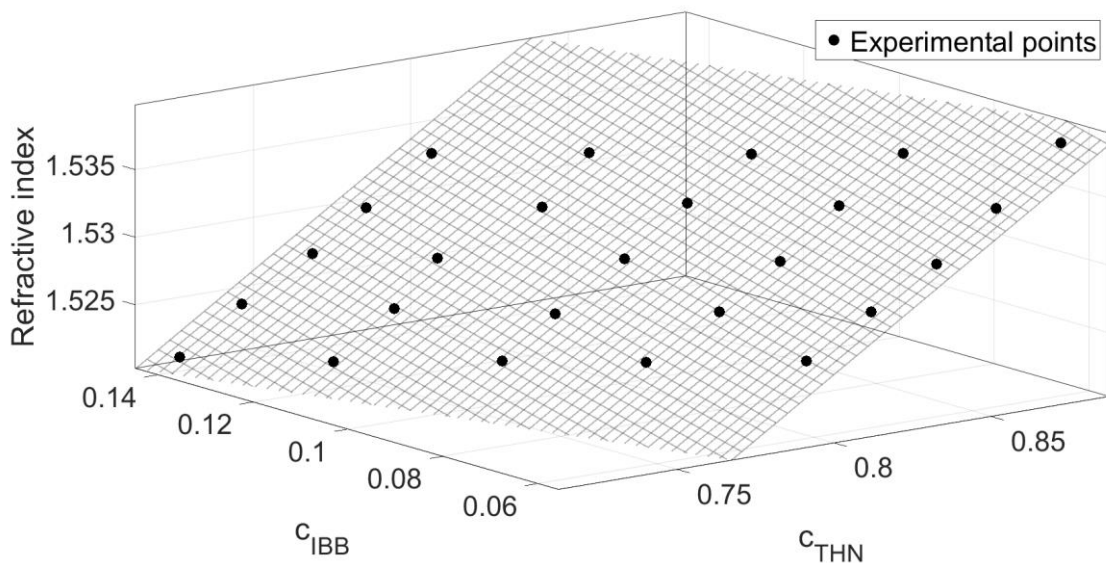
Figure 3: Fitting plane with experimental points from Table 1 at the wavelength of 480nm. C_{IBB} and C_{THN} axes represent mass fraction of isobutylbenzene and tetrahydronaphthalene respectively.

Wavelength (nm)	a_0	a_1	a_2	R^2
436	1.400	0.1589	0.10020	0.9995
480	1.397	0.1534	0.09617	0.9996
513	1.396	0.1500	0.09352	0.9996
547	1.395	0.1474	0.09145	0.9996
589	1.393	0.1448	0.08943	0.9996
633	1.393	0.1427	0.08779	0.9996
655	1.392	0.1418	0.08707	0.9996

Table 2: Fitting parameters for the refractive index function at 25°C

Refractive index field, can then be transformed into concentration in such a way

$$\frac{\partial n_i}{\partial z} = \left(\frac{\partial n_i}{\partial T}\right)_{p,c_i} \frac{\partial T}{\partial z} + \sum_{k=1}^{N} \left(\frac{\partial n_i}{\partial c_k}\right)_{p,T,c_{j\neq k}} \frac{\partial c_k}{\partial z} \quad (2)$$

by using the contrast factors $\left(\frac{\partial n_i}{\partial c_k}\right)_{p,T,c_{j\neq k}}$. In the case of microcolumn, $\frac{\partial ni}{\partial T} = 0$, as the temperature gradient is established in other direction and not z. Eq. (2) is simplified and applied to ternary mixtures into

$$\frac{\partial n_1}{\partial z} = \left(\frac{\partial n_1}{\partial c_1}\right)_{p,T,c_2} \frac{\partial c_1}{\partial z} + \left(\frac{\partial n_1}{\partial c_2}\right)_{p,T,c_1} \frac{\partial c_2}{\partial z} \quad (3)$$

$$\frac{\partial n_2}{\partial z} = \left(\frac{\partial n_2}{\partial c_1}\right)_{p,T,c_2} \frac{\partial c_1}{\partial z} + \left(\frac{\partial n_2}{\partial c_2}\right)_{p,T,c_1} \frac{\partial c_2}{\partial z} \quad (4)$$

In the matrix form along the height of the column (z) it can be written as:

$$\begin{pmatrix} \Delta n_1 \\ \Delta n_2 \end{pmatrix} = \begin{pmatrix} \frac{\partial n_1}{\partial c_1} & \frac{\partial n_1}{\partial c_2} \\ \frac{\partial n_2}{\partial c_1} & \frac{\partial n_2}{\partial c_2} \end{pmatrix} \begin{pmatrix} \Delta c_1 \\ \Delta c_2 \end{pmatrix} \quad (5)$$

with the values of the matrix easily obtained from Eq. (1). In order to calculate the concentration field, it is necessary to use the inverse of the contrast factors matrix.

$$\begin{pmatrix} \Delta c_1 \\ \Delta c_2 \end{pmatrix} = \begin{pmatrix} \frac{\partial n_1}{\partial c_1} & \frac{\partial n_1}{\partial c_2} \\ \frac{\partial n_2}{\partial c_1} & \frac{\partial n_2}{\partial c_2} \end{pmatrix}^{-1} \begin{pmatrix} \Delta n_1 \\ \Delta n_2 \end{pmatrix} \quad (6)$$

It is important to mention now that since our refractometer cannot directly determine contrast factor values for wavelength of our blue laser (473nm), it is necessary to make

an interpolation from the obtained values. To do such interpolation, the procedure explained by (Mialdun et al. 2017) is followed. This procedure correlates the change in the refractive index and contrast factors with a change in the wavelength by Cauchy dispersion. For the THN-IBB-nC12 mixture, it is concluded that the first two terms are enough to describe the change. So, it can be written

$$n(\lambda) = A_n + \frac{B_n}{\lambda^2} \quad (7)$$

$$\frac{\partial n}{\partial c_i}(\lambda) = A_{CF} + \frac{B_{CF}}{\lambda^2} \quad (8)$$

where Eqs. (7) and (8) describe the refractive index and contrast factor changes along different wavelengths respectively. A_n, B_n are the Cauchy dispersion fitting coefficients related with the fitting of refractive index values while A_{CF} and B_{CF} with the fitting contrast factor values. In particular, black lines in Figs. 4, 5 and 6 represent the Cauchy dispersion fitting using A, B values from the Table 3. Red line also represents the Cauchy dispersion fitting but using the procedure inside (Mialdun et al. 2017). Using our fitting, we can finally estimate the contrast factors at both working wavelengths. Final contrast factors values are compiled in the Table 4.
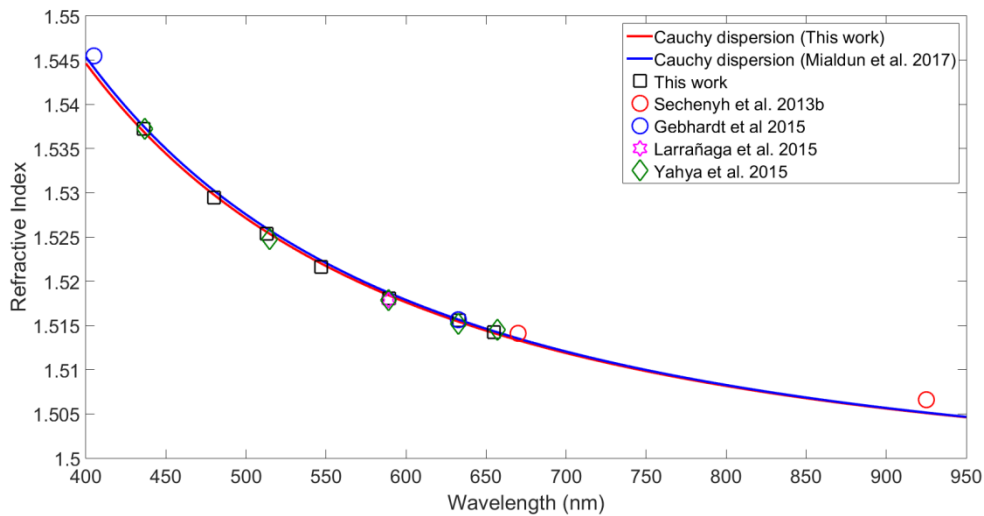

Figure 4: Refractive index of ternary mixture THN(0.8)-IBB(0.1)-nC12(0.1) with various wavelengths compared to the results reported by Mialdun et al. 2017 for mean temperature T=25°C.Symbols represent exact values reported by different groups, red circle – Sechenyh et al. 2013b, blue circle – Gebhardt et al. 2015, purple star – Larranaga et al. 2015 and green diamond – Yahya et al. 2015. Results are fitted with Eq. 7, for the values of coefficients written in Table 3.
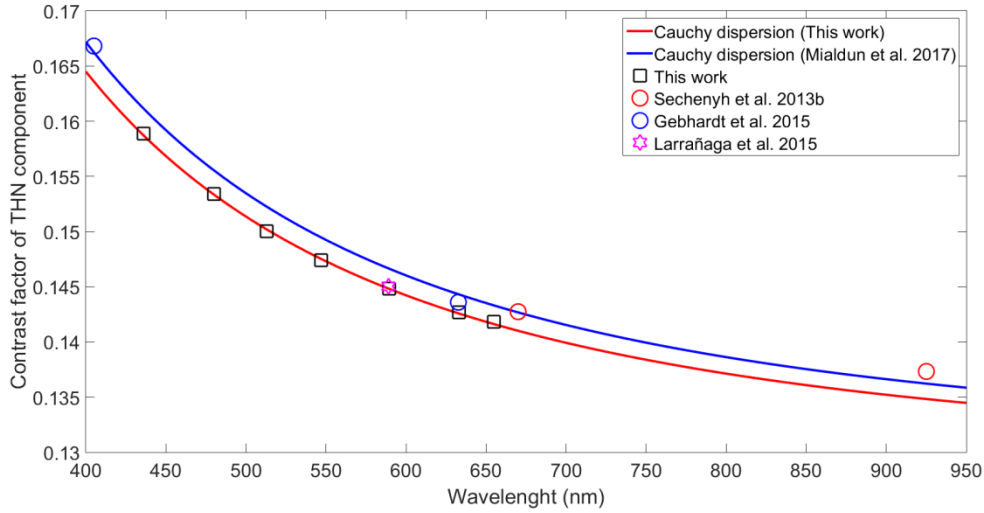
Figure 5: Contrast factor of THN (c_1) in the ternary mixture THN(0.8)-IBB(0.1)-nC12(0.1) with various wavelengths compared to the results reported by Mialdun et al. 2017 for mean temperature T=25°C. Symbols represent exact values reported by different groups, red circle – Sechenyh et al. 2013b, blue circle – Gebhardt et al. 2015, purple star – Larranaga et al. 2015. Results are fitted with Eq. (8), for the values of coefficients written in Table 3.
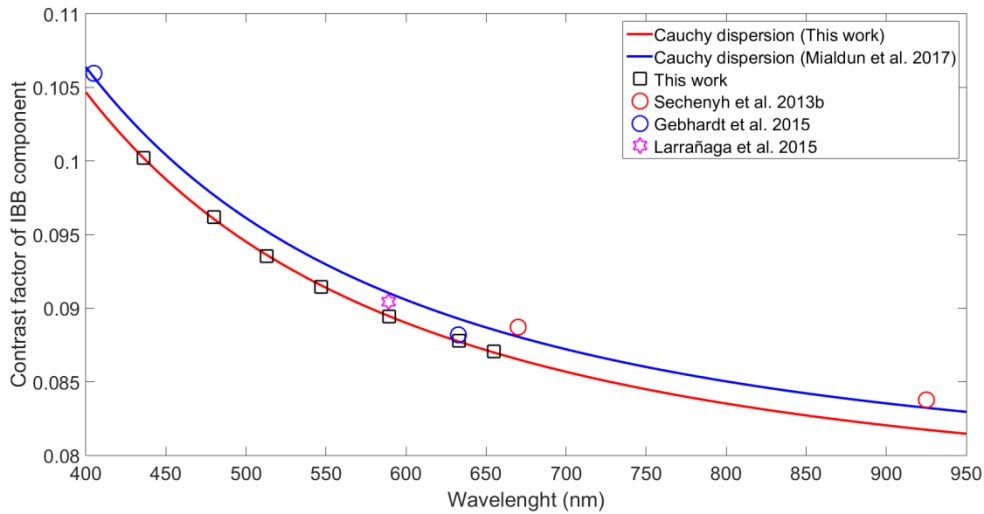

Figure 6: Contrast factor of IBB (c_2) in the ternary mixture THN(0.8)-IBB(0.1)-nC12(0.1) with various wavelengths compared to the results reported by Mialdun et al. 2017 for mean temperature T=25°C. Symbols represent exact values reported by different groups, red circle – Sechenyh et al. 2013b, blue circle – Gebhardt et al. 2015, purple star – Larranaga et al. 2015. Results are fitted with Eq. (8), for the values of coefficients written in Table 3.

Property	$A_{(nD, CF)}$	$B_{(nD, CF)}$

n_D (This work) (R^2=0.9995)	1.496	7781
n_D (Mialdun et al. 2017)	1.4959	7914
$\frac{\partial n}{\partial c_1}$ (This work) (R^2=0.9994)	0.128	5839
$\frac{\partial n}{\partial c_1}$ (Mialdun et al. 2017)	0.1291	6092
$\frac{\partial n}{\partial c_2}$ (This work) (R^2=0.9997)	0.07646	4514
$\frac{\partial n}{\partial c_2}$ (Mialdun et al. 2017)	0.0779	4557

Table 3: Fitting parameters on Cauchy dispersion of the contrast factors along different wavelengths for temperature of 25°C

Technique	$\frac{\partial n_1}{\partial c_1}$	$\frac{\partial n_1}{\partial c_2}$	$\frac{\partial n_2}{\partial c_1}$	$\frac{\partial n_2}{\partial c_2}$	Cond(N_C)
OBD (Gebhardt et.al 2015) (λ_1=405nm, λ_2=633nm)	0.16680	0.105970	0.14361	0.088186	132
ODI (Selechnyh et al. 2013) (λ_1=670nm, λ_2=925nm)	0.14271	0.088696	0.13730	0.083768	241
This work (λ_1=473nm, λ_2=633nm)	0.15409	0.096636	0.14257	0.087725	234

Table 4: Contrast factors for DCMIX1 mixture (0.8-0.1-0.1) obtained by different groups at T=25°C. Cond(N_C) represent condition number of the contrast factor matrix.

On the other hand, for the transformation into phase image, 2D Fourier Transform technique is used (Mialdun et al. 2013) once information about phase along the column windows is known, we apply

$$\Delta n(y,z) = \frac{\lambda}{2\pi d} \Delta\varphi(y,z) \qquad (9)$$

where $\Delta\varphi$ is the difference of phase along the microcolumn height, λ is the wavelength of the corresponding laser and d is the gap of the column. As there are two phase images at each point (two lasers wavelength), it means that there are refractive index difference separately for each laser applied to our system. After determination of the refractive index, using Eq. (6) it is possible to obtain the concentration field and determine the thermodiffusion coefficients.
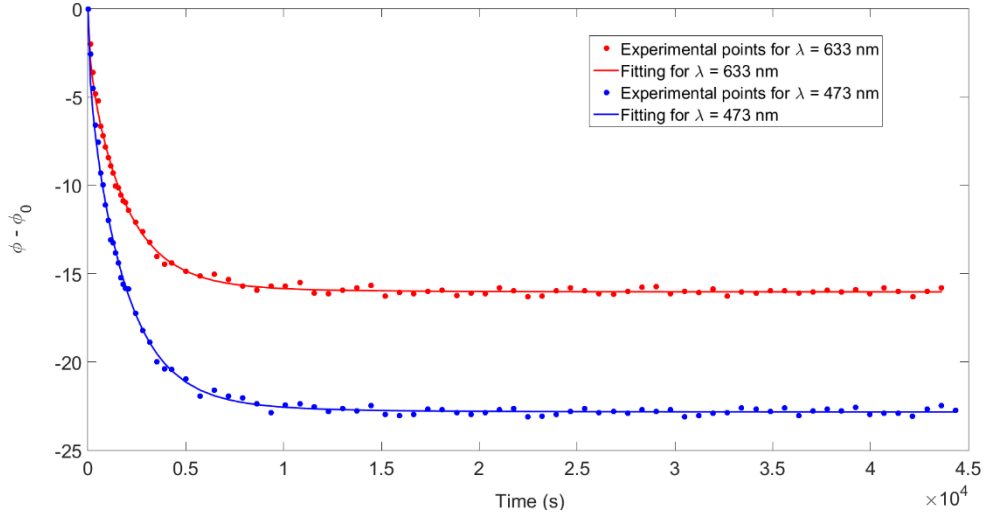
Figure 7: Time evolution of the phase difference between the point close to the top and the one close to the bottom (experiment 2 from the Table 5)

On the Figure 7 it is possible to see evolution of the phase difference along the height of microcolumn. Experiment starts usually after 2 hours of microcolumn kept on constant mean temperature which is not shown on this figure. Also, from the Eq. (9) it is clear that the shape of refractive index difference between the same points will be the same as for the phase difference. However, the uncertainty problems arise in the next step, while we are trying to determine concentration difference along the height and hence the thermodiffusion coefficients.

Determination of thermodiffusion coefficients

Thermogravitational technique relays on the Furry-Jones-Onsager theory which in ternary mixtures means that the thermodiffusion coefficients are related with the concentration difference of each component –see Eq. (10)-. This means that uncertainty from the concentration field is translated into the thermodiffusion coefficients.

$$D_{T,i}{}' = \frac{d^4 \alpha g}{504 \nu} \frac{\partial c_i}{\partial z} \qquad (10)$$

Where i (i=1,2,3) is related with each component of the mixture, d is gap of the column, g is gravitational acceleration, $\frac{\partial c_i}{\partial z}$ is the gradient of concentration along column height in the thermogravitational column in steady-state obtained by Eq. (6) and Eq. (9), α thermal diffusivity coefficient, ν is kinematic viscosity and $D_{T,i}{}'$ thermodiffusion coefficient of component i in the ternary system. Combination of thermodiffusion coefficients with molecular diffusion coefficients would result in definition of Soret coefficients in ternary mixtures $S'_{T,1}$ and $S'_{T,2}$ as (Eq. 11 and 12):

$$S'_{T,1} = \frac{D'_{T,1} D_{22} - D'_{T,2} D_{12}}{D_{11} D_{22} - D_{12} D_{21}} \qquad (11)$$

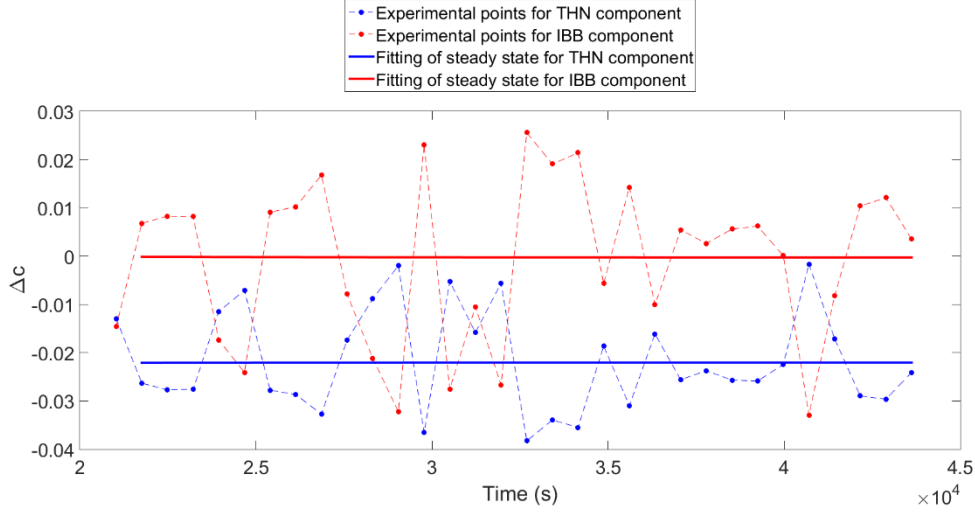$$S'_{T,2} = \frac{D'_{T,2}D_{11} - D'_{T,1}D_{21}}{D_{11}D_{22} - D_{12}D_{21}} \qquad (12)$$

Figure 8: Steady state measurement of transformed concentration field (experiment 1 from Table 5)

From Figure 8, we can see huge fluctuations in the concentration field, which are the result of ill-conditioned matrix $\frac{\partial n}{\partial c}$. The problem of the ill-conditioned matrix is not problem only related with this technique or this mixture, rather it is problem of the all optical techniques in multicomponent mixtures (Galand et al. 2019; Mialdun et al. 2017; Triller et al. 2019; Mialdun et al. 2018). Condition number, which should be as low as possible, in the case of the DCMIX1 mixture for different results is presented in the last column of the Table 4. Thermodiffusion coefficients obtained with the microcolumn are found in the Table 5:

Experiment #	$D'_{T1}\ (10^{-13})(\frac{m^2}{sK})$	$D'_{T2}\ (10^{-13})(\frac{m^2}{sK})$	$D'_{T3}\ (10^{-13})(\frac{m^2}{sK})$
1	6.89±2.74	-2.22±2.39	-4.67±0.35
2	6.94±2.76	-2.91±2.45	-4.03±0.31
Mean	6.91±2.75	-2.56±2.42	-4.35±0.33

Table 5: Thermodiffusion coefficients obtained by thermogravitational microcolumn for THN(0.8)-IBB(0.1)-nC12(0.1) mixture at T=25°C

Thermodiffusion coefficients in both experiments show good agreement, especially since this is the case of ternary mixture. Also from the Figure 9, we can see that both experiments, with small deviation are on the line of the error propagation. This means that the results obtained in this work are consistent and that dispersions from all the independent experiments would partially intersect in the proportionally large region depending on the difference between results. Thermodiffusion coefficients for the same composition from the other group can be found in the Table 6.

Technique	D'_{T1} $(10^{-13})(\frac{m^2}{sK})$	D'_{T2} $(10^{-13})(\frac{m^2}{sK})$	D'_{T3} $(10^{-13})(\frac{m^2}{sK})$
ODI+TDT (Mialdun et al. 2015)	6.9	-2.1	-4.8
OBD (Gebhardt et al. 2015)	7.2	-2.2	-5.0
TGC (Larranaga et al. 2015)	6.7	-1.8	-4.9
TGµC (This work)	6.91±2.75	-2.56±2.42	-4.35±0.33
Benchmark (Bou-Ali et al. 2015)	6.8	-2.0	-4.8

Table 6: Comparison between thermodiffusion coefficients from the literature and this work

Additionally, we run Monte Carlo simulations to bring some light on the uncertainty. Determination of the thermodiffusion coefficients is done for 100000 times for random value of Δn between $\Delta n - 0.005\Delta n$ and $\Delta n + 0.005\Delta n$. Also, calculations have been done with the results of the other groups, with contrast factor matrixes obtained in different laboratories. Thermodiffusion coefficients with its corresponding dispersion are presented on the Figure 9.
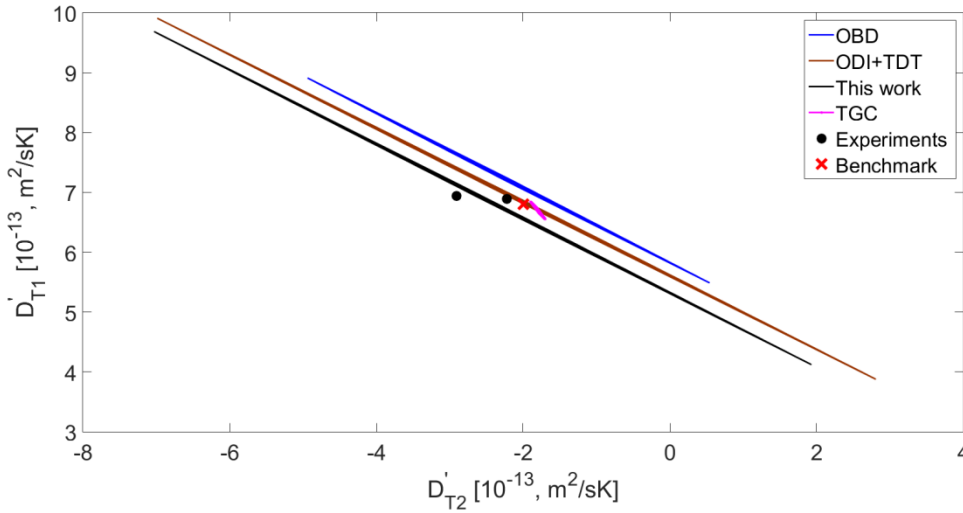

Figure 9: Thermodiffusion coefficients together with the uncertainty introduced for the mixture THN(0.8)-IBB(0.1)-nC12(0.1) at T=25°C. Results refer to the Table 6.

It is possible to note that all fully optical techniques (OBD, ODI and microcolumn) have a similar slope of coefficients dispersion. Maximum difference in the angle between those three techniques was in the case of OBD and ODI, and it was 0.4°. For that reason, those lines are almost parallel and will not intersect in the reasonable values of thermodiffusion coefficients. This is due to condition matrix nature, which in all given techniques is similar, as optical properties determined are similar. As it is possible to see from the

image, traditional thermogravitional column TGC have, due to low condition number of the contrast factor matrix, the most reliable results.

Uncertainty issues

From Figure 9, it can be noted that dispersion of D'_{T2} is higher than D'_{T1}. However, the trials to reduce the uncertainty by different choice of independent components are useless, as they will not bring higher confidence into determined thermodiffusion coefficients [29]. The condition number of the matrix with different choice, will be different, but the dispersion of the results will remain the same.

As a possible strategy to reduce the uncertainty in thermodiffusion coefficients we examined the possibility of different choices of laser wavelengths. Assuming that the nature of Cauchy dispersion fits for the most ternary mixtures it is possible to notice that the smallest condition number is related with the largest different laser wavelength difference. In this case, working laser with the minimum wavelength is from the group of Bayreuth University, with $\lambda = 405nm$ (Triller et al. 2019) and the other with maximum wavelength is from ULB group, $\lambda = 925nm$ (Galand et al. 2019). Using the values of Cauchy dispersion of this work (Table 3), condition number would be reduced to value of 96.45, which strongly reduces uncertainty in the thermodiffusion coefficients. In the Figure 10, with the red colour, dispersion of the thermodiffusion coefficients with reduced condition number are compared with the condition number dispersion experimentally obtained in this work.
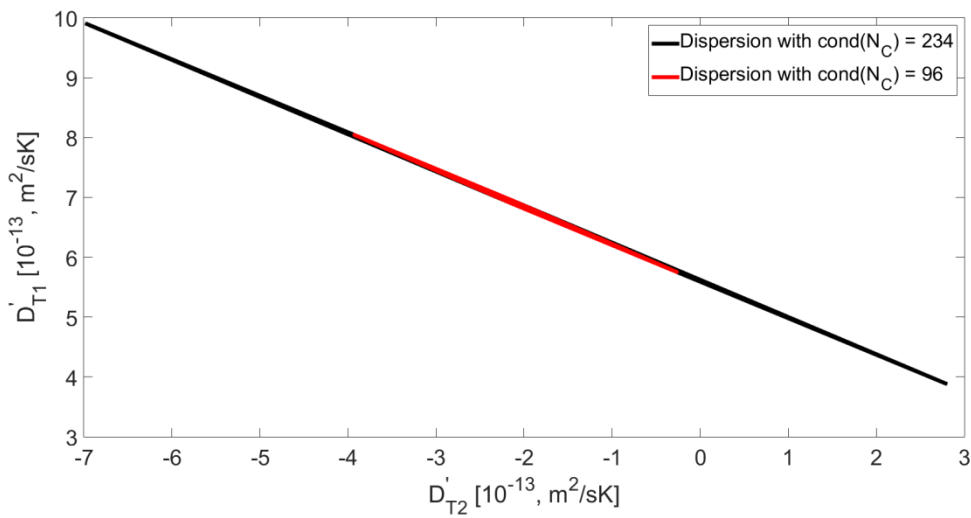

Figure 10: Dispersion of the thermodiffusion coefficients for the same error bar in the refractive index, using different contrast factor matrixes. Condition number of those matrixes is highlighted on the image.

Other possibility to reduce the uncertainty in the thermodiffusion coefficients could be the change in the slope of the dispersion direction. In this case, using multiple lasers, we could actually have intersection between dispersion curves. Slope s of the angle is related with

$$s = \frac{\frac{\partial n_1}{\partial c_1} + \frac{\partial n_2}{\partial c_1}}{\frac{\partial n_1}{\partial c_2} + \frac{\partial n_2}{\partial c_2}}. \qquad\qquad (13)$$

By applying Monte Carlo simulations using for the contrast factors obtained by Cauchy dispersion fitting, maximum and minimum angle difference in the range of wavelengths 400-950 nm is 1.1°, which is not significant to improve the accuracy. The maximum angle obtained was around 32.4°, while the minimal one was 31.3°. With such small angle difference, intersection of dispersion lines would not exist for most of the contrast factor matrixes. Moreover, the highest angle differences are usually for the small differences in laser wavelengths which would increase the condition number of the contrast factor matrix. However, as it is noticeable from the Figure 9, results from TGC have significantly different slope from the other techniques which arises from the condition number and origin of each value in the contrast factor matrix. As TGC is not fully optical technique and it relays on density measurements in ternary mixtures as well, this technique will normally have different slope than rest of the techniques. For that reason, it is important to highlight that TGC technique could provide reliable source with almost 19 times (for this mixture) smaller uncertainty in validation of thermodiffusion coefficients. For example, in the case of benchmark mixture DCMIX1, contrast factor matrix condition number is 17, and the angle between dispersion and x-axis is 36.23°. Angles related with optical techniques are: for microcolumn 31.84°, for ODI 31.62° and for OBD 32.02°, and as previously said maximum difference between those angles is just 0.4°.

The importance of a careful contrast factor measurements can be seen from the Figure 11, where we used Mialdun contrast factor matrix (Mialdun et al. 2017) and our contrast factor matrix. We simulated both cases 100000 times, in order to obtain distribution of the thermodiffusion coefficients and most expected value. From the Figure 11, but also from the Figure 9, it is noticeable that uncertainty in $D_{T,2}$ is higher than $D_{T,1}$.
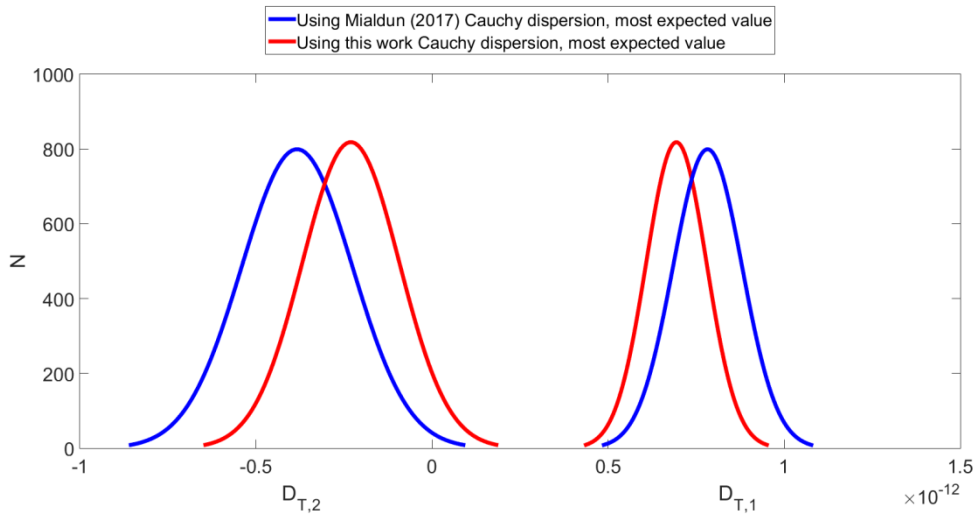

Figure 11: Distribution of the thermodiffusion coefficients using two different contrast factor matrixes, obtained using fitting parameters from Table 3

Also, from the Figure 11, we can see that results with (Mialdun et al. 2017) Cauchy dispersion values are slightly more dispersed due to slightly higher condition number for the same wavelengths.

Conclusions

In this work we successfully applied the optical digital interferometry for the ternary mixture in thermogravitational microcolumn. Thermodiffusion coefficients results obtained from the steady-state measurements coincide within 4% in the results reported in the literature in the case of D'_{T1} and within 30% in the case of D'_{T2}. However, thermogravitational column as fully optical technique faces the same problem as the other techniques in the ternary mixtures. The problem is related with the uncertainty of the obtained thermodiffusion coefficients due to ill-conditioned contrast factor matrix. In this work, we presented our contrast factor matrix for DCMIX1 mixtures and compared to those in the literature with the respect to the condition number. We proposed certain possibilities to reduce the uncertainty in the results by a careful choice of working laser wavelengths. In the end, we find very important to compare results obtained in fully optical techniques with those obtained with the traditional thermogravitational column as the TGC bring almost 19 times smaller uncertainty in results due to nature of contrast factor matrix. Moreover, the dispersion angle, which is significantly different, provides a reasonable area of intersection between the results from different groups. Future work includes transient analysis of the signal in the ternary mixtures, providing us information about eigenvalues of diffusion matrix, and if possible, individual elements of the diffusion matrix.

Conflicts of interest
There are no conflicts to declare.

Acknowledgements

References

A. Ahadi, M.Z. Saghir, The microgravity DSC-DCMIX1 mission onboard ISS: Experiment description and results on the measurement of the Soret coefficients for isobutylbenzene, dodecane, tetralin ternary hydrocarbons mixtures, Exp. Therm. Fluid Sci. 74, 296-307 (2016)

P. Blanco, M.M. Bou-Ali, J.K. Platten, D. Alonso de Mezquia, J.A. Madariaga, C.M. Santamaria, Thermodiffusion coefficients of binary and ternary hydrocarbon mixtures, J. Chem. Phys. 132(11), 114506 (2010)

M. M. Bou-Ali, O. Ecenarro, J. A. Madariaga, C. M. Santamaría, J. J. Valencia, Thermogravitational measurements of the Soret coefficient of liquid mixture, J. Phys. Condens. Matter 10, 3321-3331 (1998)

M.M. Bou-Ali, A. Ahadi, D. Alonso de Mezquia, Q. Galand, M. Gebhardt, O. Khlybov, W. Köhler, M. Larranaga, J.C. Legros, T. Lyubimova, A. Mialdun, I. Ryzhkov, M.Z. Saghir, V. Shevtsova, S. Van Vaerenbergh, Benchmark values for the Soret, thermodiffusion and molecular diffusion coefficients of the ternary mixture tetralin+isobutylbenzene+n-dodecane with 0.8-0.1-0.1 mass fraction, Eur. Phys. J. E 38 (4), 1-6 (2015)

D. Alonso De Mezquia, M. Mounir Bou-Ali, M. Larranaga, J. A. Madariaga, C. Santamaria, Determination of Molecular Diffusion Coefficient in n-Alkane Binary Mixtures: Empirical Correlations, J. Phys. Chem. B 116(9), 2814-2819 (2012)

A. Errarte, M. M. Bou-Ali, M. Aginagalde, C. Santamaria, Thermodiffusion Coefficients of Nanofluid Binary Mixtures, Microgravity Sci. Technol. 31(6), 877-882 (2019)

Q. Galand, S. Van Vaerenbergh, W. Köhler, O. Khlybov, T. Lyubimova, A. Mialdun, D. Melnikov, V. Shevtsova, T. Triller, Results of the DCMIX1 experiment on measurement of Soret coefficients in ternary mixtures of hydrocarbons under microgravity conditions on the ISS, J. Chem. Phys. 151(13), 134502 (2019)

M. Gebhardt, W. Köhler, Contribution to the benchmark for ternary mixtures: Measurement of the Soret and thermodiffusion coefficients of tetralin+isobutylbenzene+n-dodecane at a composition of (0.8/0.1/0.1) mass fraction by two-color optical beam deflection, Eur. Phys. J. E 38(4), 24 (2015)

A. Khouzam, M.-C. Charrier-Mojtabi, A. Mojtabi, B. Ouattara, A new process for species separation in a binary mixture using mixed convection. In: ICHMT Digital Library Online, Begel House Inc., Bath (2012)

A. Königer, H. Wunderlich and W. Köhler, Measurement of diffusion and thermal diffusion in ternary fluid mixtures using a two-color optical beam deflection technique, J. Chem. Phys. 132(17), 174506 (2010)

S. V. Kozlova, I. I. Ryzhkov, On the separation of multicomponent mixtures in a cylindrical thermogravitational column, Phys. Fluids 28(11), 117102 (2016)

E. Lapeira, M.M. Bou-Ali, J.A. Madariaga, C. Santamaria, Thermodiffusion coefficients of water/ethanol mixtures for low water mass fractions. Microgravity Sci. Technol. 28(5), 553-557 (2016).

E. Lapeira, M. Gebhardt, T. Triller, A. Mialdun, W. Köhler, V. Shetvsova, M.M Bou-Ali, Transport properties of the binary mixtures of the three organic liquids touluene, methanol and cyclohexane, J. Chem. Phys 146(9), 094507 (2017)

E. Lapeira, A. Mialdun, V. Yasnou, P.X. Aristimuno, V. Shevtsova, M.M. Bou-Ali, Digital Interferometry Applied to thermogravitational technique, Microgravity Sci. Technolog. 30(5), 635-641 (2018)

M. Larranaga, D. Andrew S. Rees, M.M. Bou-Ali, Determination of the molecular diffusion coefficients in ternary mixtures by sliding symmetric tubes technique, The Journal of Chemical Physics 140(5), 054201 (2014a)

M. Larranaga, M. M. Bou-Ali, E. Lapeira, C. Santamaria, J.A. Madariaga, Effect of Thermophysical Properties and Morphology of the Molecules on Thermodiffusion Coefficient of Binary Mixtures, Microgravity Sci. Technol 26(1), 29-35 (2014b)

M. Larranaga, M.M. Bou-Ali, D.A. de Mezquia, D. Andrew S. Rees, J. A. Madariaga, C. Santamaria, J.K. Platten, Contribution to the benchmark for ternary mixtures: Determination of Soret coefficients by the thermogravitational and the sliding symmetric tubes techniques, Eur. Phy. J. E 38(4), 28 (2015)

J.P. Larre, J. K. Platten, G. Chavepeyer, Soret effects in ternary systems heated from bellow, Int. J. Heat Mass Tran. 40(3), 545-555 (1997)

A. Leahy-Dios, M.M. Bou-Ali, J.K. Platten, A. Firoozabadi, Measurements of molecular and thermal diffusion coefficients in ternary mixtures, J. Chem. Phys. 122(23), 234502 (2005)

A. Martin-Mayor, M.M. Bou-Ali, M. Aginagalde, P. Urteaga, Microfluidic separation processes using the thermodiffusion effect, Int. J. Therm. Sci. 124, 279-287 (2018)

A. Mialdun, V. Shevtsova, Communication: New approach for analysis of thermodiffusion coefficients in ternary mixtures, J. Chem. Phys. 138(16), 161102 (2013)

A. Mialdun, J.C. Legros, V. Yasnou, V. Sechenyh, V. Shevtsova, Contribution to the benchmark for ternary mixtures: Measurements of the Soret, diffusion and thermodiffusion coefficients in the ternary mixture THN/IBB/nC12 with 0.8/0.1/0.1 mass fractions in ground and orbital laboratories, Eur. Phys. J. E 38(4), 27 (2015)

A. Mialdun, V. Shevtsova, Analysis of multi-wavelength measurements of diffusive properties via dispersion dependence of optical properties, Appl. Optics 56(3), 572-581 (2017)

A. Mialdun, I. Ryzhkov, O. Khlybov, T. Lyubimova, V. Shevtsova, Measurement of Soret coefficients in a ternary mixture of toluene-methanol-cyclohexane in convection-free environment, J. Chem. Phys. 148(4), 044506 (2018)

A. Mialdun, H. Bataller, M.M. Bou-Ali, M. Braibanti, F. Croccolo, A. Errarte, J. M. Ezquerro, J.J. Fernandez, Yu. Gaponenko, L. Garcia-Fernandez, J. Rodriguez, V. Shevtsova, Preliminary analysis of Diffusion Coefficient Measurements in ternary mIXtures 4 (DCMIX4) experiment on board the International Space Station, Eur. Phys. J. E 42(7), 87 (2019)

P. Naumann, A. Martin, H. Kriegs, M. Larranaga, M.M Bou-Ali, S. Wiegand, Development of a Thermogravitational Micro-column with an interferometric contracless detection system, J. Phys. Chem. B 116(47), 13889-13897 (2012)

H. Ning, S. Wiegand, Experimental investigation of the Soret effect in acetone/water and dimethylsulfoxide/water mixtures, J. Chem. Phys. 125(22), 221102 (2006)

V. Sechenyh, J.C. Legros, V. Shevtsova, Development and validation of a new setup for measurements of diffusion coefficents in ternary mixtures using the Taylor dispersion technique, CR Mechanique 341(4-5), 490-496 (2013a)

V. Sechenyh, J.C. Legros. V. Shevtsova, Optical properties of binary and ternary liquid mixtures containing tetralin, isobutylbenzene and dodecane, J. Chem. Thermodyn. 62, 64-68 (2013b)

B. Šeta, E. Lapeira, D. Dubert, F. Gavalda, M.M. Bou-Ali, X. Ruiz, Separation under thermogravitational effects in binary mixtures, Eur. Phys. J. E 42(5), 58 (2019a)

B. Šeta, A. Errarte, D. Dubert, Jna. Gavalda, M.M. Bou-Ali, X. Ruiz, Gravitational stability analysis on double diffusion convection in ternary mixtures, Acta Astronaut. 160, 442-450 (2019b)

B. Šeta, Gavaldà, Jna., Bou-Ali, M.M., Ruiz, X., Santamaria, C. (2019) Determining diffusion, thermodiffusion and Soret coefficients by the thermogravitational technique in binary Mixture with optical digital interferometry analysis, Int. J. Heat Mass Tran. 147, 118935 (2020)

T. Triller, D. Sommermann, M. Schraml, F. Sommer, E. Lapeira, M.M. Bou-Ali, W. Köhler, The Soret effect in ternary mixtures of water+ethanol+triethylene glycol of equal mass fractions: Ground and microgravity experiments, Eur. Phys. J. E 42(3), 1-11 (2019)

M. Yahya, M.Z. Saghir, Prediction and experimental measurements of refractive index in ternary hydrocarbon mixtures, J. Chem. Eng. Data 60(8), 2329-2342 (2015)